

Ab initio calculation of phonon dispersions in semiconductors

Paolo Giannozzi and Stefano de Gironcoli

*Institut Romand de Recherche Numérique en Physique des Matériaux (IRRMA), PHB-Ecublens,
CH-1015 Lausanne, Switzerland*

Pasquale Pavone and Stefano Baroni

Scuola Internazionale Superiore di Studi Avanzati (SISSA), Strada Costiera 11, I-34014 Trieste, Italy

(Received 7 August 1990)

The density-functional linear-response approach to lattice-dynamical calculations in semiconductors is presented in full detail. As an application, we calculate complete phonon dispersions for the elemental semiconductors Si and Ge, and for the III-V semiconductor compounds GaAs, AlAs, GaSb, and AlSb. Our results are in excellent agreement with experiments where available, and provide predictions where they are not. As a byproduct, we obtain real-space *interatomic* force constants for these materials, which are useful both for interpolating the dynamical matrices through the Brillouin zone, and as ingredients of approximate calculations for mixed systems such as alloys and microstructures. The possibility of studying these systems using the force constants of the pure materials relies on the so-called *mass approximation*, i.e., on neglecting the dependence of the force constants upon composition. The accuracy of such an approximation is tested and found to be very good for cationic intermixing in binary semiconductors, while it is less so for anionic substitutions. The situation is intermediate in the case of elemental semiconductors.

I. INTRODUCTION

Ab initio methods based on density-functional theory (DFT) are by now common and well established tools for studying structural and vibrational properties of real materials. The plane-wave pseudopotential method and the local-density approximation (LDA) to DFT have provided a simple framework whose accuracy and predictive power have been convincingly demonstrated in a large variety of systems.¹ The calculation of reliable phonon spectra in semiconductors is well within the reach of DFT. Recently, very efficient linear-response techniques have been proposed^{2,3} which allow one to obtain dynamical matrices at arbitrary wave vectors with a computational effort comparable to that of a self-consistent calculation for the unperturbed bulk. It is by now possible to obtain accurate phonon dispersions on a fine grid of wave vectors covering the entire Brillouin zone (BZ), which compare directly with neutron-diffraction data, and from which several physical properties of the system (such as heat capacities, thermal expansion coefficients, temperature dependence of the band gap, and so on) can be calculated.

Bulk phonon dispersion spectra are interesting not only for their relevance to properties of pure materials, but also as ingredients of approximate calculations for complex systems, such as semiconductor alloys, superlattices, and other quantum microstructures. Much attention is presently being paid to the vibrational properties of such structures, both because of their fundamental interest and as a promising tool for the structural characterization of these new materials.^{4,5} Most of the existing theoretical studies rely heavily on information about the force constants of the pure materials.⁵ Even when first-

principles calculations for the superlattice are available, bulk phonon dispersions of the constituents are very useful for interpreting the calculated spectra, and comparing them with experiments.⁶ A detailed account of disorder effects in semiconductor microstructures may require the consideration of (many) systems with a rather high number of atoms per unit cell (≈ 100 , or more). A direct first-principles calculation of the phonon spectra for such systems may be very demanding computationally, even with the highly efficient linear-response techniques presently available. On the other hand, calculations based on empirical models, such as the shell model, the bond-charge model, or others, have a limited predictive power. In fact, the parameters entering these models are fitted to experiments. In the case of AlAs, for instance, experimental information is very poor, and existing semiempirical calculations based on force constants fitted to the phonon spectrum of bulk GaAs produce a longitudinal-optic (LO) band along the ΓX direction, which is much wider than that calculated from first principles.⁶ It is therefore desirable to devise a method to treat both perfect bulk semiconductors and their alloys and microstructures with an affordable amount of computer resources, retaining an accuracy similar to that of direct first-principles calculations.

Useful information on the phonon spectra of *ordered* superlattices has been obtained making use of *interplanar force constants* calculated in an *ab initio* manner for one of the two bulk materials and taking into account the difference between the two constituents only through their different ionic masses, plus some semiempirical adjustment of the effective charges.⁷ In the case of GaAs/AlAs, a recent analysis based on first-principles calculations for the superlattice and for the two individu-

al bulks showed that similar approaches can work even better than hitherto suspected,⁸ in practice, both the bulk phonon dispersions of AIAs, and the vibrational properties of ultrathin GaAs/AIAs superlattices are closely reproduced, using the forces constants calculated for GaAs, just replacing the relevant cationic masses, *without any adjustment of the effective charges*. This observation opens the possibility of calculating the vibrational properties of very complex GaAs/AIAs structures, using the *interatomic force constants* of one of the two bulks, or possibly of the corresponding virtual crystal.^{9,10}

In this paper we present all the technical details necessary to implement the DFT linear-response approach to lattice-dynamical calculations in semiconductors,² and for calculating the corresponding interatomic force constants. As an application, we present the first *ab initio* calculation of full phonon dispersions of two elemental semiconductors, Si and Ge, and four compound semiconductors, GaAs, AlAs, GaSb, and AlSb.

Our purpose is twofold. On the one hand, by comparing our calculations with existing neutron data, we demonstrate that modern electronic-structure techniques are able to reproduce even the fine details of the phonon spectra of semiconductors, thus giving further confidence in their predictive power. In the case of AIAs, whose vibrational properties are poorly known because of the lack of neutron-scattering data, our predictions are confirmed by the excellent agreement between the phonon dispersions calculated for the closely related compound AlSb and recent neutron-scattering data.¹¹

On the other hand, we examine to what extent the interatomic force constants of the six materials are similar to each other, with a view toward using them to study the vibrational properties of mixed systems, such as alloys, superlattices (both ordered and partially disordered), or other quantum structures. In the case of III-V compounds, we find that the force constants of materials that differ by their cations are rather similar to each other, while this is less so when the materials differ by their anions. The situation is intermediate in the case of elemental semiconductors.

The paper is organized as follows. Section II contains the general method and its application to phonons in semiconductors. Section III contains our results for the bulk dispersion spectra and the force constants in real space. Section IV contains the conclusions. Several technical details are examined in the Appendixes.

II. THEORY

A. Linear response and lattice dynamics

Since the works of De Cicco and Johnson¹² and of Pick, Cohen, and Martin,¹³ it is well known that the harmonic force constants of crystals are determined by their static linear electronic response. In fact, within the adiabatic approximation, the lattice distortion associated with a phonon can be seen as a static perturbation acting on the electrons. It is a simple application of the Hellmann-Feynman theorem¹⁴ to show that the linear variation of the electron density upon application of an

external, static, perturbation determines the energy variation up to second order in the perturbation (up to third order, indeed, as shown in Ref. 15).

Suppose that the *bare* external potential acting on the electrons, V_λ (which we assume for simplicity to be local), is a continuous function of some parameters $\lambda \equiv \{\lambda_i\}$. The Hellmann-Feynman theorem states that the “force” associated with the variation of the external parameters λ is given by the ground-state expectation value of the derivative of V_λ :

$$\frac{\partial \mathcal{E}_\lambda}{\partial \lambda_i} = \int n_\lambda(\mathbf{r}) \frac{\partial V_\lambda(\mathbf{r})}{\partial \lambda_i} d\mathbf{r}, \quad (1)$$

where \mathcal{E}_λ is the electron ground-state energy relative to given values of the λ parameters, and n_λ is the corresponding electron-density distribution. Total-energy variations are obtained from Eq. (1) by integration. In order to have energy variations correct up to second order in λ , it is necessary that the right-hand side (rhs) of Eq. (1) be correct to linear order:

$$\frac{\partial \mathcal{E}_\lambda}{\partial \lambda_i} = \int \left[n_0(\mathbf{r}) \frac{\partial V_\lambda(\mathbf{r})}{\partial \lambda_i} + \sum_j \lambda_j \frac{\partial n_\lambda(\mathbf{r})}{\partial \lambda_j} \frac{\partial V_\lambda(\mathbf{r})}{\partial \lambda_i} + n_0(\mathbf{r}) \sum_j \lambda_j \frac{\partial^2 V_\lambda(\mathbf{r})}{\partial \lambda_i \partial \lambda_j} \right] d\mathbf{r} + \mathcal{O}(\lambda^2), \quad (2)$$

all the derivatives being calculated at $\lambda=0$. Integration of Eq. (2) gives

$$\begin{aligned} \mathcal{E}_\lambda = & \mathcal{E}_0 + \sum_i \lambda_i \int n_0(\mathbf{r}) \frac{\partial V_\lambda(\mathbf{r})}{\partial \lambda_i} d\mathbf{r} \\ & + \frac{1}{2} \sum_{i,j} \lambda_i \lambda_j \int \left[\frac{\partial n_\lambda(\mathbf{r})}{\partial \lambda_j} \frac{\partial V_\lambda(\mathbf{r})}{\partial \lambda_i} + n_0(\mathbf{r}) \frac{\partial^2 V_\lambda(\mathbf{r})}{\partial \lambda_i \partial \lambda_j} \right] d\mathbf{r}. \end{aligned} \quad (3)$$

Suppose now that the λ parameters represent ion displacements $u_{\alpha i}(\mathbf{R})$, where \mathbf{R} indicates the position of the unit cell, i the atomic position within the unit cell, and α is a polarization index. The matrix of the force constants is defined as

$$\begin{aligned} C_{\alpha i, \beta j}(\mathbf{R} - \mathbf{R}') &= \frac{\partial^2 \mathcal{E}}{\partial u_{\alpha i}(\mathbf{R}) \partial u_{\beta j}(\mathbf{R}')} \\ &= C_{\alpha i, \beta j}^{\text{ion}}(\mathbf{R} - \mathbf{R}') + C_{\alpha i, \beta j}^{\text{elec}}(\mathbf{R} - \mathbf{R}'), \end{aligned} \quad (4)$$

where C^{ion} is the ionic contribution to the force constants, which is essentially the second derivative of an Ewald sum whose expression is given in Appendix A; the electronic contribution C^{elec} is given by

$$\begin{aligned} C_{\alpha i, \beta j}^{\text{elec}}(\mathbf{R} - \mathbf{R}') &= \int \left[\frac{\partial n(\mathbf{r})}{\partial u_{\alpha i}(\mathbf{R})} \frac{\partial V_{\text{ion}}(\mathbf{r})}{\partial u_{\beta j}(\mathbf{R}')} \right. \\ & \quad \left. + n_0(\mathbf{r}) \frac{\partial^2 V_{\text{ion}}(\mathbf{r})}{\partial u_{\alpha i}(\mathbf{R}) \partial u_{\beta j}(\mathbf{R}')} \right] d\mathbf{r}, \end{aligned} \quad (5)$$

where $V_{\text{ion}}(\mathbf{r})$ is the *bare* ionic (pseudo) potential acting on the electrons:

$$V_{\text{ion}}(\mathbf{r}) = \sum_{\mathbf{R}, i} v_i(\mathbf{r} - \mathbf{R} - \boldsymbol{\tau}_i), \quad (6)$$

$\boldsymbol{\tau}_i$ is the position of the i th ion in the unit cell, and $\partial n(\mathbf{r})/\partial u_{ai}(\mathbf{R})$ is the electron density response to the displacement in the a th direction of the i th ion in the unit cell at \mathbf{R} . The matrix of the force constants is conveniently calculated in reciprocal space:

$$C_{ai, \beta j}(\mathbf{R}) = \frac{1}{N} \sum_{\mathbf{q}} e^{i\mathbf{q} \cdot \mathbf{R}} \tilde{C}_{ai, \beta j}(\mathbf{q}), \quad (7)$$

where N is the number of unit cells in the crystal. The electronic contribution to $\tilde{C}(\mathbf{q})$ is given by

$$\begin{aligned} \tilde{C}_{ai, \beta j}^{\text{elec}}(\mathbf{q}) = & \int \left[\frac{\partial n(\mathbf{r})}{\partial u_{aiq}} \right]^* \frac{\partial V_{\text{ion}}(\mathbf{r})}{\partial u_{\beta jq}} d\mathbf{r} \\ & + \delta_{ij} \int n_0(\mathbf{r}) \frac{\partial^2 V_{\text{ion}}(\mathbf{r})}{\partial u_{aiq=0} \partial u_{\beta jq=0}} d\mathbf{r}, \quad (8) \end{aligned}$$

where $\partial V_{\text{ion}}(\mathbf{r})/\partial u_{aiq}$ is the linear variation of the external ionic pseudopotential upon a lattice distortion of the form

$$u_{ai}(\mathbf{R}) = u_{aiq} e^{i\mathbf{q} \cdot \mathbf{R}} \quad (9)$$

and $\partial n/\partial u_{aiq}$ is the corresponding variation of the electron density.

A generalization of Eq. (8) to the case of nonlocal pseudopotentials is given in Appendix A. Equation (8) shows that the knowledge of the electron-density response to a lattice distortion of the form (9) enables one to calculate the harmonic force constants of the crystal. Phonon frequencies are then obtained by diagonalization of the

dynamical matrix, $\tilde{D}_{ai, \beta j}(\mathbf{q})$, defined as

$$\tilde{D}_{ai, \beta j}(\mathbf{q}) = \frac{\tilde{C}_{ai, \beta j}(\mathbf{q})}{(M_i M_j)^{1/2}}, \quad (10)$$

where the M 's are ionic masses.

B. Density-functional linear response

Recently, very powerful techniques have been developed to calculate the electronic linear response of periodic systems in the framework of DFT.² These techniques have been successfully applied to zone-center phonons of elemental and binary semiconductors,¹⁶ and of semiconductor superlattices.⁶ Here we present them in the general case of perturbations of arbitrary wavelength.

The self-consistent-field (SCF) DFT potential V_{SCF} for a system of electrons moving in the external potential of the ions is given by

$$V_{\text{SCF}}(\mathbf{r}) = V_{\text{ion}}(\mathbf{r}) + e^2 \int \frac{n(\mathbf{r}')}{|\mathbf{r} - \mathbf{r}'|} d\mathbf{r}' + v_{\text{XC}}(n(\mathbf{r})), \quad (11)$$

and can be determined by standard techniques of self-consistent band-structure calculations. Let us superimpose to the ionic potential a perturbation ΔV_{bare} of given periodicity \mathbf{q} . The self-consistent potential will change accordingly: $V_{\text{SCF}} \rightarrow V_{\text{SCF}} + \Delta V_{\text{SCF}}$. For the sake of clarity, in this section, we use a description in terms of finite differences: the passage to the description in terms of derivatives—which is used in the rest of the paper—is straightforward. If ΔV_{SCF} is supposed to be known, the linear variation in the electron density Δn is obtained by first-order perturbation theory:

$$\Delta \bar{n}(\mathbf{q} + \mathbf{G}) = \frac{4}{N\Omega} \sum_{\mathbf{k}} \sum_{c, v} \frac{\langle \psi_{v, \mathbf{k}} | e^{-i(\mathbf{q} + \mathbf{G}) \cdot \mathbf{r}} | \psi_{c, \mathbf{k} + \mathbf{q}} \rangle \langle \psi_{c, \mathbf{k} + \mathbf{q}} | \Delta V_{\text{SCF}} | \psi_{v, \mathbf{k}} \rangle}{\epsilon_{v, \mathbf{k}} - \epsilon_{c, \mathbf{k} + \mathbf{q}}} \quad (12)$$

where $\Delta \bar{n}(\mathbf{q} + \mathbf{G})$ is the Fourier transform of $\Delta n(\mathbf{r})$, Ω is the volume of the unit cell, v and c indicate valence and conduction bands, respectively, and the sum over \mathbf{k} covers the first Brillouin zone. It is here assumed that the crystal has doubly occupied valence bands and empty conduction bands separated by a gap. On the other hand, if Δn is known, ΔV_{SCF} can be obtained by linearizing Eq. (11):

$$\begin{aligned} \Delta V_{\text{SCF}}(\mathbf{r}) = & \Delta V_{\text{bare}}(\mathbf{r}) + e^2 \int \frac{\Delta n(\mathbf{r}')}{|\mathbf{r} - \mathbf{r}'|} d\mathbf{r}' \\ & + \Delta n(\mathbf{r}) \left[\frac{dv_{\text{XC}}}{dn} \right]_{n=n_0(\mathbf{r})}, \quad (13) \end{aligned}$$

where n_0 is the unperturbed electron density. Equations (12) and (13) form a system that can be solved iteratively. It should be remarked that the linear response to a perturbation of given \mathbf{q} only contains Fourier components of wave vector $\mathbf{q} + \mathbf{G}$; different \mathbf{q} 's do not mix at this order of perturbation theory.

For computational convenience, it is desirable to avoid the sum over conduction bands of Eq. (12). This can be achieved by rewriting Eq. (12) in the following way:

$$\begin{aligned} \Delta \bar{n}(\mathbf{q} + \mathbf{G}) = & \frac{4}{N\Omega} \sum_{\mathbf{k}} \sum_v \langle \psi_{v, \mathbf{k}} | e^{-i(\mathbf{q} + \mathbf{G}) \cdot \mathbf{r}} P_c \\ & \times G(\epsilon_{v, \mathbf{k}}) P_c \Delta V_{\text{SCF}}^q | \psi_{v, \mathbf{k}} \rangle, \quad (14) \end{aligned}$$

where P_c is the projector over the conduction-state manifold, $G(\epsilon) = 1/(\epsilon - H_{\text{SCF}})$ is the one-electron Green's function of the unperturbed system, and the superscript in ΔV_{SCF}^q has been introduced to stress that ΔV_{SCF} —when acting on a wave function of wave vector \mathbf{k} —transforms it into a function of wave vector $\mathbf{k} + \mathbf{q}$. Note that no special difficulties arise in evaluating Eq. (14) when ΔV_{SCF}^q is a nonlocal operator. To evaluate Eq. (14), we further rewrite it as

$$\Delta\bar{n}(\mathbf{q}+\mathbf{G}) = \frac{4}{N\Omega} \sum_{\mathbf{k}} \sum_{\nu} \langle \psi_{\nu,\mathbf{k}} | e^{-i(\mathbf{q}+\mathbf{G})\cdot\mathbf{r}} P_c | \Delta\psi_{\nu,\mathbf{k}+\mathbf{q}} \rangle, \quad (15)$$

where $\Delta\psi_{\nu,\mathbf{k}+\mathbf{q}}$ is solution of the linear system:

$$[\varepsilon_{\nu,\mathbf{k}} - H_{\text{SCF}}] | \Delta\psi_{\nu,\mathbf{k}+\mathbf{q}} \rangle = P_c \Delta V_{\text{SCF}}^{\mathbf{q}} | \psi_{\nu,\mathbf{k}} \rangle. \quad (16)$$

The linear system (16) has an infinite number of solutions because the determinant of $[\varepsilon_{\nu,\mathbf{k}} - H_{\text{SCF}}]$ vanishes, and the vector on the left-hand side (lhs) is orthogonal to the null space of $[\varepsilon_{\nu,\mathbf{k}} - H_{\text{SCF}}]$. In practice, $\Delta\psi_{\nu,\mathbf{k}+\mathbf{q}}$ is defined within a multiple of $\psi_{\nu,\mathbf{k}}$. As $\Delta\psi_{\nu,\mathbf{k}+\mathbf{q}}$ enters Eq. (15) only through its projection onto the conduction-state manifold, such an indeterminacy does not affect the final result. Depending on the size of the basis set, Eq. (16) can be solved either by factorization techniques,¹⁷ or by iterative methods. In both cases, the calculation of all the needed functions $\Delta\psi_{\nu,\mathbf{k}+\mathbf{q}}$ requires a numerical labor comparable to that needed for a single SCF iteration for the *unperturbed* system.

The method described in this section applies to a general perturbation. The matrix elements necessary when the perturbation describes a lattice distortion are given in Appendix B.

C. Polar semiconductors

1. Nonanalyticity at small wavelengths

In polar semiconductors, the long-range character of the Coulomb forces gives rise to macroscopic electric fields for LO phonons in the limit $\mathbf{q} \rightarrow 0$. For finite \mathbf{q} , polar semiconductors are dealt with in the same way as nonpolar ones. In the long-wavelength limit, however, the macroscopic electric field \mathbf{E} , which accompanies the lattice distortion must be treated with care because the corresponding electronic potential $\Phi(\mathbf{r}) = -\mathbf{E}\cdot\mathbf{r}$, is not lattice-periodic. Within linear-response theory, electric fields can be dealt with during the self-consistent process performed to determine the density response to ionic displacements.² A more convenient way of dealing with long-wavelength vibrations in polar semiconductors is to exploit the known analytic properties of the dynamical matrix. In the long-wavelength limit, the matrix of the force constants can be written as the sum of analytic and nonanalytic contributions:^{18,19}

$$\tilde{C}_{ai,\beta j} = \tilde{C}_{ai,\beta j}^{\text{an}} + \tilde{C}_{ai,\beta j}^{\text{na}}, \quad (17)$$

where the analytic part \tilde{C}^{an} is the matrix obtained from the response to a zone-center phonon, calculated with electric boundary conditions (EBC) corresponding to zero macroscopic electric field (*zero* EBC). *Zero* EBC are implicitly assumed in any electronic-structure calculations with periodic boundary conditions for the electronic wave functions. The nonanalytic part has the general form¹⁹

$$\begin{aligned} \tilde{C}_{ai,\beta j}^{\text{na}} &= \frac{4\pi e^2}{\Omega} \frac{\sum_{\gamma} Z_{i,\gamma\alpha}^* q_{\gamma} \sum_{\nu} Z_{j,\nu\beta}^* q_{\nu}}{\sum_{\gamma,\nu} q_{\gamma} \varepsilon_{\gamma\nu}^{\infty} q_{\nu}} \\ &= \frac{4\pi e^2}{\Omega} \frac{(\mathbf{q}\cdot\mathbf{Z}_i^*)_{\alpha} (\mathbf{q}\cdot\mathbf{Z}_j^*)_{\beta}}{\mathbf{q}\cdot\tilde{\varepsilon}^{\infty}\cdot\mathbf{q}}, \end{aligned} \quad (18)$$

where $\varepsilon_{\alpha\beta}^{\infty}$ is the high-frequency static dielectric tensor (i.e., the electronic contribution to the static dielectric tensor), and $Z_{i,\alpha\beta}^*$ is the Born effective charge tensor for the i th atom in the unit cell. Equation (18) shows that all the information necessary to deal with the nonanalytic part of the dynamical matrix is contained in the macroscopic dielectric constant of the system and in the Born effective charges \mathbf{Z}^* , whereas the analytic contribution can be calculated by just ignoring any macroscopic polarization associated with the phonon. All these quantities can be easily obtained within our framework.

2. Calculation of the dielectric tensor

The dielectric tensor relates the screened electric field (with clamped nuclei) \mathbf{E} to the bare electric field \mathbf{E}_0 : $\mathbf{E}_0 = \tilde{\varepsilon}^{\infty} \cdot \mathbf{E}$. The matrix elements of the bare electrostatic potential $\Phi_0(\mathbf{r}) = -\mathbf{E}_0 \cdot \mathbf{r}$ are ill-defined in an infinite solid with periodic boundary conditions. They can be cast in a boundary-insensitive form by using the following relation:²⁰

$$\langle \psi_{c,\mathbf{k}} | \mathbf{r} | \psi_{v,\mathbf{k}} \rangle = \frac{\langle \psi_{c,\mathbf{k}} | [H_{\text{SCF}}, \mathbf{r}] | \psi_{v,\mathbf{k}} \rangle}{\varepsilon_{v,\mathbf{k}} - \varepsilon_{c,\mathbf{k}}}, \quad (19)$$

where

$$[H_{\text{SCF}}, \mathbf{r}] = \frac{-i\hbar\mathbf{p}}{m} + [V_{\text{ion}}, \mathbf{r}], \quad (20)$$

\mathbf{p} is the momentum operator, and m is the electron mass. For a finite system, Eq. (19) is an identity. When periodic boundary conditions are used, however, the lhs is no longer well defined, whereas the rhs is still so and does not present any problem when passing to the thermodynamic limit. Note that commutator $[V_{\text{ion}}, \mathbf{r}]$ does not vanish if the electron-ion interaction is described by a nonlocal potential, as is the case in the calculations presented below (see Appendix B). For practical purposes, we calculate once and for all and store the auxiliary functions:

$$\begin{aligned} |\phi_{v,\mathbf{k}}^{\alpha}\rangle &= P_c r_{\alpha} | \psi_{v,\mathbf{k}} \rangle = \sum_c |\psi_{c,\mathbf{k}}\rangle \frac{\langle \psi_{c,\mathbf{k}} | [H, r_{\alpha}] | \psi_{v,\mathbf{k}} \rangle}{\varepsilon_{c,\mathbf{k}} - \varepsilon_{v,\mathbf{k}}} \\ &= -P_c G_0(\varepsilon_{v,\mathbf{k}}) P_c [H, r_{\alpha}] | \psi_{v,\mathbf{k}} \rangle. \end{aligned} \quad (21)$$

When an external electric field is applied, the bare perturbing potential has only a macroscopic ($\mathbf{G}=0$) component, whereas the screened potential has both macroscopic and microscopic ($\mathbf{G}\neq 0$) components. The latter are given as usual by Eqs. (13) and (14). The former is proportional to the electronic contribution to the macroscopic polarization per unit volume \mathbf{P} :²¹

$$\frac{\partial \mathbf{P}}{\partial E_{\alpha}} = \frac{e}{N\Omega} \int \mathbf{r} \frac{\partial n(\mathbf{r})}{\partial E_{\alpha}} d\mathbf{r}, \quad (22)$$

which can be recast into the form^{21,22}

$$\frac{\partial \mathbf{P}}{\partial E_\alpha} = \frac{4e}{N\Omega} \sum_{\mathbf{k}} \sum_{c,v} \frac{\langle \psi_{v,\mathbf{k}} | \mathbf{r} | \psi_{c,\mathbf{k}} \rangle \langle \psi_{c,\mathbf{k}} | (\partial V_{\text{SCF}} / \partial E_\alpha) | \psi_{v,\mathbf{k}} \rangle}{\epsilon_{v,\mathbf{k}} - \epsilon_{c,\mathbf{k}}}. \quad (23)$$

This result can be equivalently obtained by considering the density response to a perturbation of finite wave vector \mathbf{q} :

$$\Delta n(\mathbf{r}) = e^{i\mathbf{q}\cdot\mathbf{r}} \sum_{\mathbf{G}} C_{\mathbf{G}}(\mathbf{q}) e^{i\mathbf{G}\cdot\mathbf{r}}.$$

It is easy to see that, for small \mathbf{q} , one has $C_{\mathbf{G}=\mathbf{0}}(\mathbf{q}) \approx -i\mathbf{q}\cdot\mathbf{P}$, and obtain from this Eq. (23). Equation (23) is well defined and boundary insensitive,²¹ provided that the matrix elements of \mathbf{r} are dealt with as prescribed by Eq. (19).

Equation (23) can be used to obtain the screened electric field $\mathbf{E} = \mathbf{E}_0 - 4\pi\mathbf{P}$ at each iteration of the self-consistent process. However, for computational purposes, it is more convenient to keep the value of the screened electric field fixed during self-consistency, and let only the microscopic components of the potential vary. The macroscopic polarization is then calculated from Eq. (23), once self-consistency is achieved. Physically, this amounts to calculating the polarization response to a given *screened* electric field \mathbf{E} instead of to the *bare* electric field \mathbf{E}_0 .

Let us introduce the following notation for the response of the wave function $|\psi_{v,\mathbf{k}}\rangle$ to an applied screened electric field:

$$\left| \frac{\partial \psi_{v,\mathbf{k}}}{\partial E_\beta} \right\rangle = P_c G_0(\epsilon_{v,\mathbf{k}}) P_c \frac{\partial V_{\text{SCF}}}{\partial E_\beta} |\psi_{v,\mathbf{k}}\rangle, \quad (24)$$

where $\partial V_{\text{bare}}(\mathbf{r}) / \partial E_\beta = -r_\beta$. The induced polarization is obtained through Eq. (23) and the dielectric tensor $\tilde{\epsilon}^\infty$ is finally given by

$$\epsilon_{\alpha\beta}^\infty = \delta_{\alpha\beta} + \frac{16\pi e^2}{N\Omega} \sum_{\mathbf{k}} \sum_v \left\langle \phi_{v,\mathbf{k}}^\alpha \left| \frac{\partial \psi_{v,\mathbf{k}}}{\partial E_\beta} \right\rangle \right\rangle. \quad (25)$$

3. Calculation of the Born effective charges

The calculation of the Born effective charges proceeds along similar lines. The Born effective charges are simply related to the total (ionic + electronic) macroscopic polarization \mathbf{P}^{tot} induced by a zone-center phonon with zero EBC:^{22,23}

$$\mathbf{Z}_{i,\alpha\beta}^* = \frac{\Omega}{e} \frac{\partial P_\alpha^{\text{tot}}}{\partial u_{\beta i \mathbf{q}=\mathbf{0}}}, \quad (26)$$

where $u_{\beta i \mathbf{q}=\mathbf{0}}$ is the amplitude of the zero-center phonon, as defined by Eq. (9). The ionic contribution to the polarization is trivial, whereas the electronic contribution is obtained from the linear response to a zone-center phonon as in Eq. (23). In our notations one has

$$\mathbf{Z}_{i,\alpha\beta}^* = \mathbf{Z}_i + \frac{4}{N} \sum_{\mathbf{k}} \sum_v \left\langle \phi_{v,\mathbf{k}}^\alpha \left| \frac{\partial \psi_{v,\mathbf{k}}}{\partial u_{\beta i \mathbf{q}=\mathbf{0}}} \right\rangle \right\rangle, \quad (27)$$

where \mathbf{Z}_i is the bare ionic (pseudo)charge of the i th ion and $\partial \psi / \partial u$ is the linear variation of the electronic wave function, upon lattice distortion.

D. Real-space interatomic force constants

In nonpolar materials (such as elemental semiconductors) the range of the interatomic forces constants defined by Eq. (4) is short. For this reason, interatomic force constants offer a convenient way of storing the information contained in the dynamical matrices $\bar{D}_{\alpha i, \beta j}(\mathbf{q})$ at any \mathbf{q} into a few (typically some tens) independent parameters. Real-space force constants are conveniently calculated by Fourier analyzing their reciprocal-space counterpart, Eq. (7), calculated onto a finite grid. The number of force constants so obtained is equal to the number of \mathbf{q} points in the finite grid, the maximum range being essentially given by $2\pi/\Delta q$, where Δq is the discretization parameter of the reciprocal-space grid. Once real-space constants have been obtained in this way, reciprocal-space dynamical matrices can be calculated by inverse Fourier transform at any point of the BZ (i.e., even at a point not contained in the original grid). For this reason, real-space force constants are a powerful tool for interpolating dynamical matrices throughout the BZ.

In polar material (such as compound semiconductors), the range of the interatomic force constants is not short anymore, due to dipolar interactions associated with non-vanishing effective charges. Mathematically, the long-range character of the force constants is the origin of the nonanalytic behavior of $\tilde{C}(\mathbf{q})$, as $\mathbf{q} \rightarrow \mathbf{0}$. As the nonanalytic part of $\tilde{C}(\mathbf{q})$ can be expressed in terms of the ionic effective charges and dielectric tensor of the system through Eq. (18), the former is easily separated out of $\tilde{C}(\mathbf{q})$, once ϵ_∞ and the \mathbf{Z}^* 's have been calculated. Once this is done, the remaining analytic term can be treated as in nonpolar materials.

Note that subtracting Eq. (18) from the matrix of the force constants, $\tilde{C}(\mathbf{q})$, and expressing the resulting difference in terms of real-space force constants, effectively maps the lattice-dynamical problem onto a rigid-ion model whose interaction constants, however, are not necessarily restricted to a small number of neighbors.

III. RESULTS

A. Technicalities

Our calculations are performed in the framework of the LDA plane-wave pseudopotential method. The exchange-correlation energy and potential are taken from Ref. 24. We have generated norm-conserving pseudopotentials using a scheme proposed by von Barth and Car,²⁵ and paying particular attention to the choice of reference configuration for atomic d states, which were found to be rather important for ensuring the correct lattice mismatch among the different semiconductors. Plane

waves up to a kinetic-energy cutoff of 16 Ry have been used. These basis sets are complete enough to guarantee a convergence on the calculated phonon frequencies of better than 5 cm^{-1} . The sums over electronic eigenstates in the BZ have been performed using ten Chadi-Cohen \mathbf{k} points in the irreducible wedge.²⁶ Dynamical matrices have been then calculated onto a (444) reciprocal space fcc grid.²⁷ Fourier deconvolution on this mesh yields real-space interatomic force constants up to the ninth shell of neighbors. This procedure is equivalent to calculating real-space force constants using an fcc supercell whose linear dimensions are four times larger than the primitive zinc-blende cell, thus containing 128 atoms. A direct SCF calculation on such a supercell would require a numerical effort proportional to the third power of the number of atoms, whereas our linear-response approach requires an effort proportional to the number of \mathbf{q} points in the reciprocal-space grid, and hence to the number of atoms in the supercell.

Phonon frequencies along low-symmetry lines have been obtained interpolating the dynamical matrices using the above force constants, as described in Sec. II D. Along the high-symmetry lines Δ (Γ - X) and Λ (Γ - L) we have calculated the dynamical matrices at additional points [all those belonging to the (888) fcc mesh]. One-dimensional Fourier analysis of the dynamical matrices yields the *interplanar* force constants. Interpolation of the dynamical matrices using these *interplanar* force constants gives the same phonon dispersion that would be obtained from a full three-dimensional calculation onto a (888) fcc mesh. Optical branches are found to be insensitive to the choice between the two meshes, whereas the (888) mesh turns out to improve somewhat the agreement of our calculated dispersions with experiment, in the acoustic region. For polar materials, the long-range interaction, which was implicitly eliminated by subtracting the nonanalytic part of $\tilde{C}(\mathbf{q})$, before Fourier analysis, was restored using an Ewald sum similar to that used to evaluate \tilde{C}^{ion} , as explained in Appendix A 1 [see Eq. (A6), where the ionic charges Z_i have to be replaced by $Z_i^*/\sqrt{\epsilon^\infty}$].

B. Bulk dispersions and comparison with experiments

In Table I we report the values of the lattice parameters used for calculating the phonon spectra of the six materials we have investigated, along with the calculated values of the effective charges and dielectric constants,

which have been used for treating long-wavelength modes. Similar values for these quantities had been obtained in a previous paper¹⁶ by the same technique, but using different pseudopotentials. As expected, the differences are quite small. The reported values of the effective charges are obtained by imposing the acoustic sum rule (ASR):

$$\sum_i Z_{i,\alpha\beta}^* = 0. \quad (28)$$

In approximate calculations, the ASR is violated. The magnitude of such a violation strongly depends on the mesh of \mathbf{k} points used for the sum over the BZ: it is large if few \mathbf{k} points are used, and tends to zero as the size of the mesh increases. Notwithstanding, if the ASR is imposed by subtracting from each effective charge one-half of their sum, good results are obtained with few \mathbf{k} points, and the data reported in Table I should be considered as converged to the figures quoted. The values of the dielectric constants are overestimated with respect to experiments by $\approx 10\%$. This is a well-known drawback of the LDA known for a certain time^{20(a)} and discussed in some detail in Ref. 16.

Our results for the bulk phonon dispersions along several symmetry lines, together with the corresponding densities of state, are displayed in Figs. 1 and 2, for non-polar and polar materials, respectively. Some numerical values at the high-symmetry points Γ , X , and L are also reported in Table II. Many neutron-diffraction and Raman-scattering data^{11,28-33} are available for all the semiconductors considered here, with the exception of AlAs, for which only a few Raman experiments exist.³¹ The agreement between calculations and available experiments is excellent. This is of particular importance in view of the fact that we believe this to be the first time that phonon dispersions of real materials have been calculated completely from first principles, throughout the entire Brillouin zone. In the case of AlAs, where a direct comparison with experiment is not possible, our calculation is a reliable prediction of the phonon dispersions. Previous calculations were, in fact, either limited to very few high-symmetry points,³⁴ or based on semiempirical models that were fitted to the phonon dispersions of GaAs. Our calculations predict that the AlAs LO branch along the Δ direction is much flatter than hitherto suspected. This fact, which is relevant for understanding the physics of phonons in GaAs/AlAs superlattices,⁶ seems to be confirmed by the agreement between our calculations and the available experimental data at the X

TABLE I. Equilibrium lattice parameter [a , (a.u.)] used in the present calculations, calculated Born effective charges (Z^*), and static dielectric constants (ϵ_∞). Parentheses denote experimental data.

	Si	Ge	GaAs	AlAs	GaSb	AlSb
a	10.20 (10.26)	10.60 (10.68)	10.605 (10.68)	10.605 (10.69)	11.40 (11.49)	11.51 (11.58)
Z^*			2.07 (2.07)	2.17 (2.18)	1.73 (1.88)	1.91 (2.18)
ϵ_∞	13.6 (12.1)	18.7 (16.5)	12.3 (10.9)	9.2 (8.2)	18.1 (14.4)	12.2 (10.2)

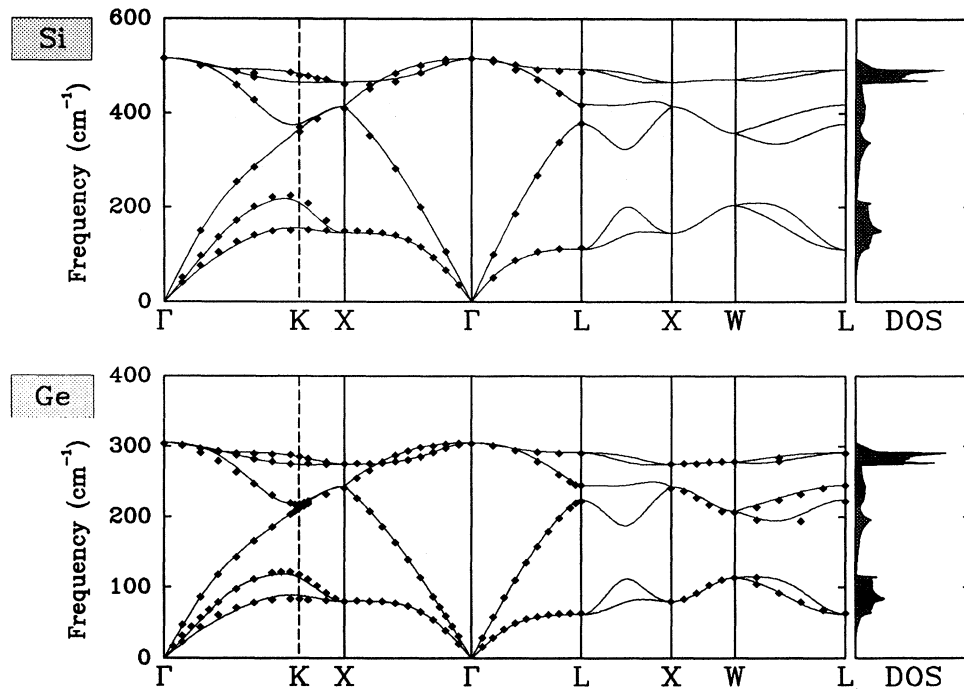


FIG. 1. Calculated phonon dispersions and densities of state of elemental semiconductors, Si and Ge. Experimental data are denoted by diamonds (from Refs. 28 and 29).

point.^{31(b)} The reliability of those experimental data are, however, somewhat questionable, and the agreement perhaps fortuitous. More meaningful is that the reliability of the present prediction for AIAs is confirmed by the good agreement between our calculations and recent experiments for the closely related compound AlSb.¹¹ Even in the case of GaAs, for which phonon dispersions along the high-symmetry Δ and Λ lines had already been calculated using *interplanar* force constants,³⁵ the present calculations represent an important step forward both because they have been performed for many more (low-

symmetry) directions, and also because they are considerably more accurate, resulting in a much better agreement with experiment. This is particularly so in what concerns effective charges and LO-TO splittings, and the flatness of the TA branch near the X point. Finally, it is worth noting that, in the case of GaAs, also the predicted vibrational eigendisplacements at the X and L points are in good agreement with experiment (see Table III), and with previous theoretical calculations.^{35,36} The main features of our method, which have made possible these improvements, are the following. First of all, our Green's-

TABLE II. Phonon frequencies calculated at the high-symmetry points Γ , X, and L, for the six materials considered in this work (cm^{-1}). Experimental data are in parentheses. Data tagged with an asterisk are from Ref. 33.

	Si ^a	Ge ^b	GaAs ^c	AIAs ^d	GaSb ^e	AlSb ^f
Γ_{TO}	517 (517)	306 (304)	271 (271)	363 (361)	230 (224)*	316 (323)*
Γ_{LO}	517 (517)	306 (304)	291 (293)	400 (402)	237 (233)*	334 (344)*
X_{TA}	146 (150)	80 (80)	82 (82)	95 (109)	57 (57)	64 (70)
X_{LA}	414 (410)	243 (241)	223 (225)	216 (219)	162 (166)	153 (155)
X_{TO}	466 (463)	275 (276)	254 (257)	337 (333)	210 (212)	290 (296)
X_{LO}	414 (410)	243 (241)	240 (240)	393 (399)	211 (212)	343 (341)
L_{TA}	111 (114)	62 (63)	63 (63)	71	45 (46)	49 (56)
L_{LA}	378 (378)	224 (222)	210 (207)	212	157 (153)	149 (148)
L_{TO}	494 (487)	291 (290)	263 (264)	352	203 (205)	306 (308)
L_{LO}	419 (417)	245 (245)	238 (242)	372	221 (216)	327 (320)

^a Experimental data from Ref. 28.

^b Experimental data from Ref. 29.

^c Experimental data from Ref. 30.

^d Experimental data from Ref. 31.

^e Experimental data from Ref. 32.

^f Experimental data from Ref. 11.

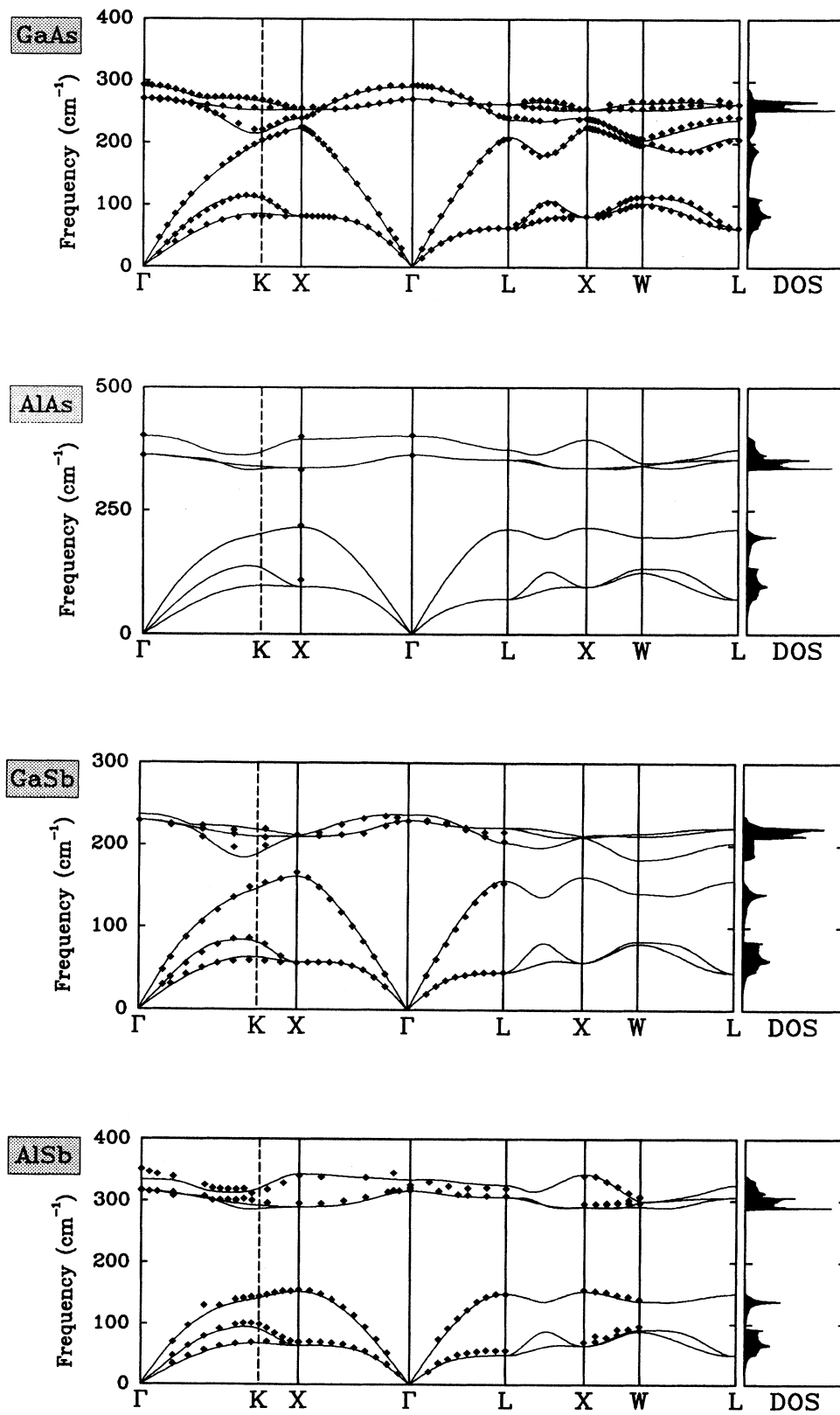


FIG. 2. Calculated phonon dispersions and densities of state for binary semiconductors, GaAs, AlAs, GaSb, and AlSb. Experimental data are denoted by diamonds (from Refs. 30–32 and 11).

TABLE III. Vibrational eigenvectors at the X and L points of the Brillouin zone for III-V semiconductors. e is the cationic component of the optic mode. The indexes L and T indicate longitudinal and transverse modes, respectively. The experimental data reported in parentheses are from Ref. 30.

	GaAs	AlAs	GaSb	AlSb
$e_T(X)$	0.66	0.85	0.91	0.77
$e_T(L)$	0.70	0.86	0.91	0.79
$e_L(X)$	1 (1)	1	1	1
$e_L(L)$	0.74 (0.56 or 0.81)	0.99	0.97	1.00

function technique avoids the use of supercells, thus allowing us to calculate force constants of longer range, not limited to the high-symmetry directions; still, accurate, norm-conserving (nonlocal, instead of local) pseudopotentials can be used without special difficulties; last but not least the overall numerical efficiency of our method allows us to use a high number of special points and large plane-wave basis-sets, thus permitting us to obtain fully converged results.

C. Transferability of the force constants

The qualitative behavior of the real-space force constants calculated for Si and Ge is similar to that previously obtained by dielectric matrices and local pseudopotentials.³⁷ In particular, we have found that the force constants decay slowly in the direction of the bond chains, $\langle 110 \rangle$. A similar behavior has been observed also in III-V compounds, once the long-range tails of the force constants are removed, as discussed in Sec. II D.

We wish now to assess to what extent the force constants calculated for one material are able to describe the lattice dynamics of another material or a mixture of the two (such as an alloy or a microstructure). To this end, we have calculated the phonon dispersions of several materials using the dynamical matrices obtained for different materials that differ from the former for the cationic or anionic species. Our results are displayed in Fig. 3, where the notation $[A] \rightarrow B$ indicates that phonons of material B have been obtained with the dynamical matrix calculated for material A at its equilibrium lattice parameter, uniquely replacing the relevant masses (*mass approximation*). In the case of GaAs and AlAs, which differ for the cationic species and have practically the same lattice parameter, the mass approximation gives phonon dispersions practically indistinguishable from the real ones in the acoustical and transverse optic regions, while they differ by less than 10 cm^{-1} in the LO region. Such an accuracy is achieved without any empirical adjustment of the effective charges. In fact, the small discrepancies are almost entirely due to the small difference between the effective charges of the two materials. It turns out that *ab initio* force constants calculated for GaAs are indeed capable of describing rather accurately phonon dispersions in AlAs, while semiempirical dynamical matrices (such as those from the bond-charge or other models), fitted to the GaAs dispersions, give an AlAs LO band

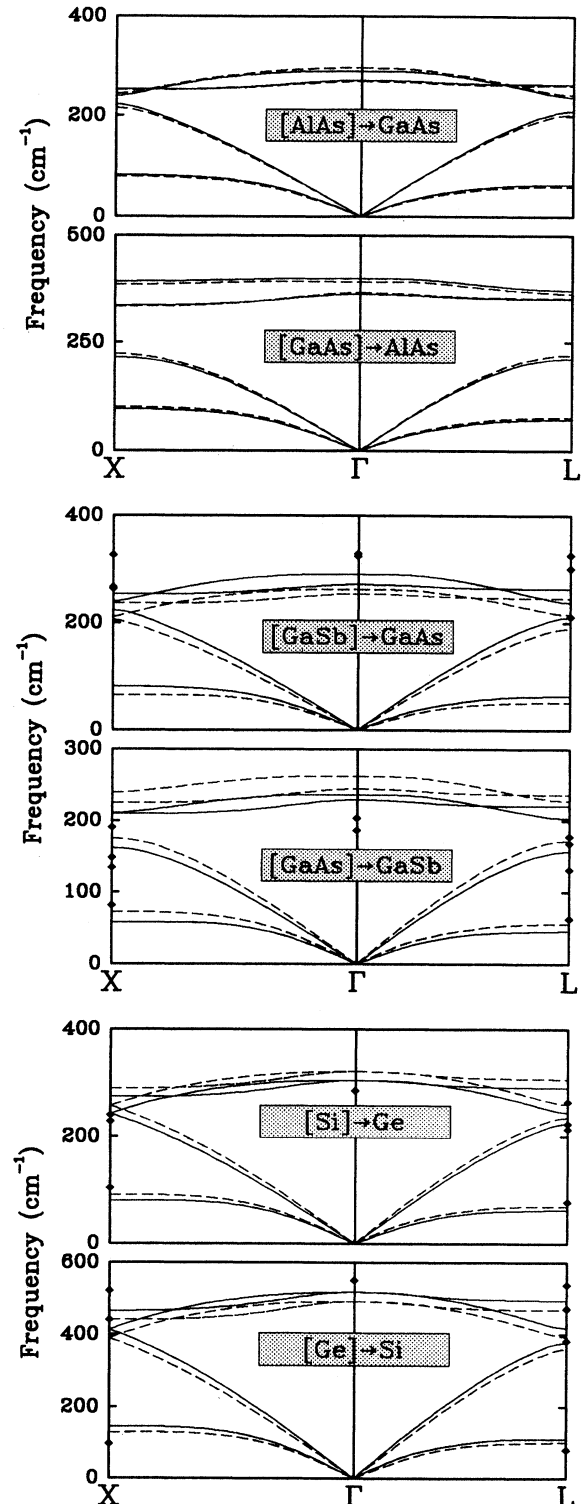


FIG. 3. Comparison between the phonon dispersions calculated with (dashed line) and without (solid line) the mass approximation. The notation $[A] \rightarrow B$ indicates that phonon dispersions of material B have been obtained with the dynamical matrix appropriate to material A , replacing just the relevant masses. The diamonds indicate the frequencies obtained calculating the dynamical matrices of material A at the lattice parameter appropriate for material B .

width along ΓX , which is quite a bit larger than that calculated from first principles. This indicates that the agreement between the calculated frequencies and experiments is by no means a sufficient criterion for judging the quality of a model. A similar accuracy is also obtained for Sb compounds, where the lattice mismatch is larger. These results clearly indicate that the use of the mass approximation for systems that differ for the cationic species is well justified, provided accurate force constants are used.

In the case of GaAs and GaSb (which differ for the anionic species and have a rather large lattice mismatch) the mass approximation gives poorer results, with errors larger than 30 cm^{-1} . This fact had been already remarked and attributed to the larger polarizability of the anions.³⁸ One could think that the main source of inaccuracy lies in the large lattice mismatch. To verify this issue, we have also calculated some representative phonon frequencies for system B , using the force constants of system A , calculated at the lattice parameter of system B . The results are indicated by diamonds at the X , Γ , and L points in Fig. 3. We see that even worse results are obtained in this case. Similar results have been obtained for Al compounds as well. We conclude that the mass approximation is much less accurate when the systems differ by their anions than when they differ by their cations.³⁸ Finally, in the case of Si and Ge, the accuracy of the mass approximation is somewhat intermediate between the above two cases, as expected.

IV. CONCLUSIONS

In this paper we have shown that the accurate calculation of complete phonon dispersions of semiconductors is by now well within the scope of computational methods based on density-functional theory. The results so obtained compare very favorably with experiment. The concept of *interatomic* force constants is very useful, not only for interpolating vibrational properties throughout the Brillouin zone, but also for using the information gained in simple systems (such as elemental or binary semiconductors) in rather complex ones, such as alloys and quantum structures; this is feasible in a straightforward way in the case of pseudobinary systems presenting different cationic species, and, to a minor extent, for Si/Ge. Applications of these ideas to GaAs/AlAs and

Si/Ge systems are in fact under way, with very promising preliminary results. The case of pseudobinary systems with different anions may require some semiempirical adjustment of the force constants, in order to achieve a comparable accuracy.

ACKNOWLEDGMENTS

This work has been cosponsored by the Italian Ministry of the University and Scientific Research through the collaborative project between SISSA and the CINECA supercomputing center, by the Italian Consiglio Nazionale della Ricerche under Grant No. 89.00006.69, by the Swiss National Science Foundation under Grant No. 20-5446.87, and by the European Research Office of the U.S. Army under Grant No. DAJA 45-89-C-0025.

APPENDIX A: EXPRESSION OF THE FORCE CONSTANTS

1. Electronic term, nonlocal potentials

If the electron-ion interaction is described by a nonlocal potential, Eqs. (1) and (3) do not hold and one must use the more general expressions

$$\frac{\partial \mathcal{E}_\lambda}{\partial \lambda_i} = \sum_{\mathbf{k}} \sum_{\nu} \left\langle \psi_{\nu, \mathbf{k}} \left| \frac{\partial V_\lambda}{\partial \lambda_i} \right| \psi_{\nu, \mathbf{k}} \right\rangle \quad (\text{A1})$$

and

$$\begin{aligned} \frac{\partial^2 \mathcal{E}_\lambda}{\partial \lambda_i \partial \lambda_j} = & \sum_{\mathbf{k}} \sum_{\nu} \left[\left\langle \psi_{\nu, \mathbf{k}} \left| \frac{\partial^2 V_\lambda}{\partial \lambda_i \partial \lambda_j} \right| \psi_{\nu, \mathbf{k}} \right\rangle \right. \\ & + \left\langle \frac{\partial \psi_{\nu, \mathbf{k}}}{\partial \lambda_i} \left| \frac{\partial V_\lambda}{\partial \lambda_j} \right| \psi_{\nu, \mathbf{k}} \right\rangle \\ & \left. + \left\langle \psi_{\nu, \mathbf{k}} \left| \frac{\partial V_\lambda}{\partial \lambda_j} \right| \frac{\partial \psi_{\nu, \mathbf{k}}}{\partial \lambda_i} \right\rangle \right]. \quad (\text{A2}) \end{aligned}$$

The first term is a ‘‘diagonal’’ term, which can be calculated without any knowledge of the response of the system; the last two terms (which are equal due to time-reversal symmetry) need only the knowledge of the linear response of the system.

In \mathbf{q} space, the two contributions have the form

$$\begin{aligned} \bar{C}_{ai, \beta j}^{(1)}(\mathbf{q}) &= \frac{2}{N} \sum_{\mathbf{R}, \mathbf{R}'} \sum_{\mathbf{k}} \sum_{\nu} \left\langle \psi_{\nu, \mathbf{k}} \left| \frac{\partial^2 V_{\text{ion}}}{\partial u_{ai}(\mathbf{R}) \partial u_{\beta j}(\mathbf{R}')} \right| \psi_{\nu, \mathbf{k}} \right\rangle e^{-i\mathbf{q} \cdot (\mathbf{R} - \mathbf{R}')} \\ &= \delta_{ij} \frac{2}{N} \sum_{\mathbf{k}} \sum_{\nu} \left\langle \psi_{\nu, \mathbf{k}} \left| \frac{\partial^2 V_{\text{ion}}}{\partial u_{ai\mathbf{q}=0} \partial u_{\beta i\mathbf{q}=0}} \right| \psi_{\nu, \mathbf{k}} \right\rangle \end{aligned} \quad (\text{A3})$$

and

$$\bar{C}_{ai, \beta j}^{(2)}(\mathbf{q}) = \frac{4}{N} \sum_{\mathbf{R}, \mathbf{R}'} \sum_{\mathbf{k}} \sum_{\nu} \left\langle \frac{\partial \psi_{\nu, \mathbf{k}}}{\partial u_{ai}(\mathbf{R})} \left| \frac{\partial V_{\text{ion}}}{\partial u_{\beta j}(\mathbf{R}')} \right| \psi_{\nu, \mathbf{k}} \right\rangle e^{-i\mathbf{q} \cdot (\mathbf{R} - \mathbf{R}')} = \frac{4}{N} \sum_{\mathbf{k}} \sum_{\nu} \left\langle \frac{\partial \psi_{\nu, \mathbf{k}}}{\partial u_{ai\mathbf{q}}} \left| \frac{\partial V_{\text{ion}}}{\partial u_{\beta j\mathbf{q}}} \right| \psi_{\nu, \mathbf{k}} \right\rangle. \quad (\text{A4})$$

A factor of 2 comes from the spin summation. The first term does not depend on \mathbf{q} and can be calculated only once.

2. Ionic term

The ionic term in the force constants arises from the ion-ion Ewald term:

$$\begin{aligned} \mathcal{E}_{\text{Ewald}} = & \frac{4\pi N e^2}{\Omega} \frac{1}{2} \left[\sum_{(\mathbf{G} \neq 0)} \frac{e^{-G^2/4\alpha}}{G^2} \left| \sum_l \mathbf{Z}_l e^{i\mathbf{G} \cdot \boldsymbol{\tau}_l} \right|^2 - \frac{1}{4\alpha} \left(\sum_l \mathbf{Z}_l \right)^2 \right] \\ & + \frac{Ne^2}{2} \sum_{l,m} \sum_{\mathbf{R}} \frac{\mathbf{Z}_l \mathbf{Z}_m}{|\boldsymbol{\tau}_l - \boldsymbol{\tau}_m - \mathbf{R}|} [1 - \text{erf}(\sqrt{\alpha} |\boldsymbol{\tau}_l - \boldsymbol{\tau}_m - \mathbf{R}|)] - Ne^2 \left(\frac{2\alpha}{\pi} \right)^{1/2} \sum_l \mathbf{Z}_l^2, \end{aligned} \quad (\text{A5})$$

where \mathbf{Z}_i indicates the bare ionic (pseudo)charges for the i th atom, and α is a parameter whose arbitrary value can be chosen large enough to allow the neglect of the real-space term. After some tedious but straightforward algebra one finds

$$\begin{aligned} \tilde{C}_{ai,\beta j}^{\text{ion}}(\mathbf{q}) = & \frac{4\pi e^2}{\Omega} \sum_{\mathbf{G}, \mathbf{q} + \mathbf{G} \neq 0} \frac{e^{-(\mathbf{q} + \mathbf{G})^2/4\alpha}}{(\mathbf{q} + \mathbf{G})^2} \mathbf{Z}_i \mathbf{Z}_j e^{i(\mathbf{q} + \mathbf{G}) \cdot (\boldsymbol{\tau}_i - \boldsymbol{\tau}_j)} (q_\alpha + G_\alpha)(q_\beta + G_\beta) \\ & - \frac{2\pi e^2}{\Omega} \sum_{\mathbf{G} \neq 0} \frac{e^{-G^2/4\alpha}}{G^2} \left[\mathbf{Z}_i \sum_l \mathbf{Z}_l e^{i\mathbf{G} \cdot (\boldsymbol{\tau}_i - \boldsymbol{\tau}_l)} G_\alpha G_\beta + \text{c.c.} \right] \delta_{ij}. \end{aligned} \quad (\text{A6})$$

Note that, when the bare nuclear charges in Eq. (A6) are replaced by the corresponding effective charges $\mathbf{Z}_i^*/(\epsilon^\infty)^{1/2}$, Eq. (A6) is identical to the matrix of Coulomb coefficients appearing in rigid-ion models.

APPENDIX B: MATRIX ELEMENTS

Let us consider the matrix elements between plane waves

$$\langle \mathbf{r} | \mathbf{k} + \mathbf{G} \rangle = \frac{1}{\sqrt{N\Omega}} e^{i(\mathbf{k} + \mathbf{G}) \cdot \mathbf{r}} \quad (\text{B1})$$

of the various quantities needed. The electron-ion interaction is given by a nonlocal pseudopotential of the usual form

$$v_i(\mathbf{r}, \mathbf{r}') = v_{i,\text{loc}}(r) \delta(\mathbf{r} - \mathbf{r}') + \sum_l v_{i,l}(\mathbf{r}, \mathbf{r}'), \quad (\text{B2})$$

where

$$v_{i,l}(\mathbf{r}, \mathbf{r}') = \frac{2l+1}{4\pi} v_{i,l}(r) P_l(\hat{\mathbf{r}} \cdot \hat{\mathbf{r}}') \delta(r - r'), \quad (\text{B3})$$

where P_l is the Legendre polynomial of degree l . The plane-wave matrix elements of the above operator are given by

$$\begin{aligned} \langle \mathbf{k} + \mathbf{G} | v_i | \mathbf{k} + \mathbf{G}' \rangle \\ = \tilde{v}_{i,\text{loc}}(\mathbf{G} - \mathbf{G}') + \sum_l \tilde{v}_{i,l}(\mathbf{k} + \mathbf{G}, \mathbf{k} + \mathbf{G}'), \end{aligned} \quad (\text{B4})$$

where

$$\tilde{v}_{i,\text{loc}}(\mathbf{G}) = \frac{1}{\Omega} \int v_{i,\text{loc}}(r) e^{-i\mathbf{G} \cdot \mathbf{r}} d\mathbf{r}, \quad (\text{B5})$$

and

$$\begin{aligned} \tilde{v}_{i,l}(\mathbf{k}_1, \mathbf{k}_2) = & \frac{1}{\Omega} \int e^{-i\mathbf{k}_1 \cdot \mathbf{r}} v_{i,l}(\mathbf{r}, \mathbf{r}') e^{i\mathbf{k}_2 \cdot \mathbf{r}'} d\mathbf{r} d\mathbf{r}' \\ = & \frac{4\pi}{\Omega} (2l+1) P_l(\hat{\mathbf{k}}_1 \cdot \hat{\mathbf{k}}_2) \\ & \times \int_0^\infty r^2 j_l(k_1 r) j_l(k_2 r) v_{i,l}(r) dr. \end{aligned} \quad (\text{B6})$$

The matrix elements of the bare perturbations are

$$\begin{aligned} \left\langle \mathbf{k} + \mathbf{q} + \mathbf{G} \left| \frac{\partial V_{\text{ion}}}{\partial u_{aiq}} \right| \mathbf{k} + \mathbf{G}' \right\rangle \\ = -i(q_\alpha + G_\alpha - G'_\alpha) e^{-i(\mathbf{q} + \mathbf{G} - \mathbf{G}') \cdot \boldsymbol{\tau}_i} \\ \times \left[\tilde{v}_{i,\text{loc}}(\mathbf{q} + \mathbf{G} - \mathbf{G}') \right. \\ \left. + \sum_l \tilde{v}_{i,l}(\mathbf{k} + \mathbf{q} + \mathbf{G}, \mathbf{k} + \mathbf{G}') \right]. \end{aligned} \quad (\text{B7})$$

The screening contribution to $\partial V_{\text{SCF}}/\partial u_{aiq}$, which is a local potential in DFT, can be advantageously evaluated in real space and transformed back to reciprocal space by fast-Fourier transform. The matrix elements of the second derivative of the electron-ion interaction potential are given by

$$\begin{aligned} \left\langle \mathbf{k} + \mathbf{G} \left| \frac{\partial^2 V_{\text{ion}}}{\partial u_{aiq=0} \partial u_{\beta i q=0}} \right| \mathbf{k} + \mathbf{G}' \right\rangle \\ = -(\mathbf{G}_\alpha - \mathbf{G}'_\alpha)(\mathbf{G}_\beta - \mathbf{G}'_\beta) e^{-i(\mathbf{G} - \mathbf{G}') \cdot \boldsymbol{\tau}_i} \\ \times \left[\tilde{v}_i(\mathbf{G} - \mathbf{G}') + \sum_l \tilde{v}_{i,l}(\mathbf{k} + \mathbf{G}, \mathbf{k} + \mathbf{G}') \right]. \end{aligned} \quad (\text{B8})$$

The matrix elements of the nonlocal pseudopotential contribution to $[H, \mathbf{r}]$ between plane waves are

$$\begin{aligned}
\langle \mathbf{k}_1 | [v_{i,l}, r_\alpha] | \mathbf{k}_2 \rangle &= \frac{1}{\Omega} \int e^{-i\mathbf{k}_1 \cdot \mathbf{r}} v_{i,l}(\mathbf{r}, \mathbf{r}') (r'_\alpha - r_\alpha) e^{i\mathbf{k}_2 \cdot \mathbf{r}'} d\mathbf{r} d\mathbf{r}' \\
&= -i \left[\frac{\partial}{\partial k_{1\alpha}} + \frac{\partial}{\partial k_{2\alpha}} \right] \frac{1}{\Omega} \int e^{-i\mathbf{k}_1 \cdot \mathbf{r}} v_{i,l}(\mathbf{r}, \mathbf{r}') e^{i\mathbf{k}_2 \cdot \mathbf{r}'} d\mathbf{r} d\mathbf{r}' \\
&= -i \left[\frac{\partial}{\partial k_{1\alpha}} + \frac{\partial}{\partial k_{2\alpha}} \right] \bar{v}_{i,l}(\mathbf{k}_1, \mathbf{k}_2).
\end{aligned} \tag{B9}$$

- ¹For a recent review, see, for instance, W. E. Pickett, *Comput. Phys. Rep.* **9**, 115 (1989).
- ²S. Baroni, P. Giannozzi, and A. Testa, *Phys. Rev. Lett.* **58**, 1861 (1987).
- ³For an independent derivation of the technique exposed in Ref. 2, see also N. E. Zein, *Fiz. Tverd. Tela. Leningrad* **26**, 3028 (1984) [*Sov. Phys.—Solid State* **26**, 1825 (1984)]. A hybrid linear-response-supercell method for lattice-dynamical calculations has also been developed by D. King-Smith and R. J. Needs, *J. Phys. Condens. Matter* **2**, 3431 (1990).
- ⁴For a recent review, see, for instance, B. Jusserand and M. Cardona, in *Light Scattering in Solids V*, edited by M. Cardona and G. Güntherodt (Springer, Berlin, 1989), p. 49.
- ⁵See A. Fasolino and E. Molinari, *Surf. Sci.* **228**, 112 (1990), and references quoted therein.
- ⁶S. Baroni, P. Giannozzi, and E. Molinari, *Phys. Rev. B* **41**, 3870 (1990).
- ⁷E. Molinari and A. Fasolino, *Superlattices Microstruct.* **4**, 449 (1988).
- ⁸E. Molinari, S. Baroni, P. Giannozzi, and S. de Gironcoli, in *Light Scattering in Semiconductor Structures and Superlattices, NATO Advanced Study Institute, Series B: Physics*, edited by D. J. Lockwood and J. F. Young (Plenum, New York, in press).
- ⁹S. Baroni, S. de Gironcoli, and P. Giannozzi, *Phys. Rev. Lett.* **65**, 84 (1990).
- ¹⁰E. Molinari, S. Baroni, P. Giannozzi, and S. de Gironcoli (unpublished).
- ¹¹D. Strauch, B. Dorner, and K. Karch, in *Proceedings of the Third International Conference on Phonon Physics, Heidelberg, 1989*, edited by S. Hunklinger, W. Ludwig, and G. Weiss (World Scientific, Singapore, 1990), p. 82.
- ¹²P. D. De Cicco and F. A. Johnson, *Proc. R. Soc. London Ser. A* **310**, 111 (1969).
- ¹³R. Pick, M. H. Cohen, and R. M. Martin, *Phys. Rev. B* **1**, 910 (1970).
- ¹⁴H. Hellmann, *Einführung in die Quantenchemie* (Deuticke, Leipzig, 1937); R. P. Feynman, *Phys. Rev.* **56**, 340 (1939).
- ¹⁵X. Gonze and J. P. Vigneron, *Phys. Rev. B* **39**, 13 120 (1989).
- ¹⁶S. de Gironcoli, S. Baroni, and R. Resta, *Phys. Rev. Lett.* **62**, 2843 (1989).
- ¹⁷If factorization techniques are used, the best choice is to first tridiagonalize H_{SCF} and then solve the system in the basis where it is tridiagonal. The advantage to this is that it allows one to perform just one factorization for *all* the systems corresponding to different values of $\varepsilon_{\mathbf{v},\mathbf{k}}$.
- ¹⁸M. Born and K. Huang, *Dynamical Theory of Crystal Lattices* (Oxford University Press, Oxford, 1954).
- ¹⁹W. Cochran and R. A. Cowley, *J. Chem. Phys. Solids* **23**, 447 (1962).
- ²⁰S. Baroni and R. Resta, *Phys. Rev. B* **33**, 7017 (1986); M. S. Hybertsen and S. G. Louie, *ibid.* **35**, 5585 (1987).
- ²¹P. Giannozzi, S. de Gironcoli, and R. Resta, in *Proceedings of the Third International Conference on Phonon Physics, Heidelberg, 1989* (Ref. 11), p. 205.
- ²²P. B. Littlewood, *J. Phys. C* **13**, 4893 (1980).
- ²³P. Vogl, *J. Phys. C* **11**, 251 (1978).
- ²⁴J. Perdew and A. Zunger, *Phys. Rev. B* **23**, 5048 (1981).
- ²⁵U. von Barth and R. Car (unpublished). This scheme consists essentially of a fitting minimization of the squared differences between the atomic all-electron and pseudoeigenvalues and eigenfunctions (beyond a given core radius r_c), as functions of a few parameters upon which the pseudopotential depends.
- ²⁶D. J. Chadi and M. L. Cohen, *Phys. Rev. B* **8**, 5747 (1973).
- ²⁷We define the (LMN) reciprocal-space fcc grid as the set of points $\mathbf{q}_{lmn} = (l/L)\mathbf{G}_1 + (m/M)\mathbf{G}_2 + (n/N)\mathbf{G}_3$, $\mathbf{G}_1, \mathbf{G}_2, \mathbf{G}_3$ being a basis of the reciprocal space of an fcc lattice, and $0 \leq l < L - 1, 0 < m < M - 1, 0 \leq n < N - 1$.
- ²⁸G. Dolling, in *Inelastic Scattering of Neutrons in Solids and Liquids*, edited by S. Eklund (IAEA, Vienna, 1963), Vol. II, p. 37; G. Nilsson and G. Nelin, *Phys. Rev. B* **6**, 3777 (1972).
- ²⁹G. Nilsson and G. Nelin, *Phys. Rev. B* **3**, 364 (1971).
- ³⁰D. Strauch and B. Dorner, *J. Phys. Condens. Matter* **2**, 1457 (1990).
- ³¹(a) A. Onton, in *Proceedings of the 10th International Conference on the Physics of Semiconductors, Cambridge, Massachusetts, 1970*, edited by S. P. Keller, J. C. Heusel, and F. Stern (U.S. Atomic Energy Commission, New York, 1970), p. 107; (b) B. Monemar, *Phys. Rev. B* **8**, 5711 (1973).
- ³²M. K. Farr, J. G. Traylor, and S. K. Sinha, *Phys. Rev. B* **11**, 1587 (1975).
- ³³A. Mooradin and G. B. Wright, *Solid State Commun.* **4**, 431 (1966).
- ³⁴The only previous *ab initio* calculations on phonons in AlAs are by K. J. Chang and M. L. Cohen, in *Proceedings of the 17th International Conference on the Physics of Semiconductors, San Francisco, 1984*, edited by J. D. Chadi and W. A. Harrison (Springer, New York, 1985), p. 1151. This calculation only provides results for TO(Γ), and X modes.
- ³⁵K. Kunc and R. M. Martin, in *Ab Initio Calculation of Phonon Spectra*, edited by J. T. Devreese, V. E. van Doren, and P. E. van Camp (Plenum, New York, 1983), p. 65.
- ³⁶K. Kunc and P. Hagège, in *Phonon Physics*, edited by J. Kollár, N. Kroó, N. Menyhard, and T. Siklós (World Scientific, Singapore, 1985), p. 943.
- ³⁷A. Fleszar and R. Resta, *Phys. Rev. B* **34**, 7140 (1986).
- ³⁸N. Meskini and K. Kunc, Université Pierre et Marie Curie, Technical Report No. 5, 1978 (unpublished).